ISSN 1063-780X, Plasma Physics Reports, 2007, Vol. 33, No. 7, pp. 602–612. © Pleiades Publishing, Ltd., 2007.
Original Russian Text © N.K. Berezhetskaya, V.A. Kop'ev, I.A. Kossyi, N.I. Malykh, M.A. Misakyan, M.I. Taktakishvili, S.M. Temchin, Young Dong Lee, 2007, published in Fizika Plazmy, 2007, Vol. 33, No. 7, pp. 661–672.

LOW-TEMPERATURE PLASMA

Resonance Microwave Volume Plasma Source

N. K. Berezhetskaya[a], V. A. Kop'ev[a], I. A. Kossyi[a], N. I. Malykh[a], M. A. Misakyan[a], M. I. Taktakishvili[a], S. M. Temchin[a], and Young Dong Lee[b]

[a] *Prokhorov Institute of General Physics, Russian Academy of Sciences, ul. Vavilova 38, Moscow, 119991 Russia*

[b] *Samsung Advanced Institute of Technology, Mt. 14-1, Nongseo-dong, Giheung-gu, Yongin-si Gyunggi-do, 446-712 South Korea*

Received September 21, 2006

Abstract—A conceptual design of a microwave gas-discharge plasma source is described. The possibility is considered of creating conditions under which microwave energy in the plasma resonance region would be efficiently converted into the energy of thermal and accelerated (fast) electrons. Results are presented from interferometric and probe measurements of the plasma density in a coaxial microwave plasmatron, as well as the data from probe measurements of the plasma potential and electron temperature. The dynamics of plasma radiation was recorded using a streak camera and a collimated photomultiplier. The experimental results indicate that, at relatively low pressures of the working gas, the nonlinear interaction between the microwave field and the inhomogeneous plasma in the resonance region of the plasmatron substantially affects the parameters of the ionized gas in the reactor volume.

PACS numbers: 52.50.Dg, 52.80.Pi

DOI: 10.1134/S1063780X07070094

1. INTRODUCTION

The aim of the present work was to design and investigate a new type of microwave gas-discharge plasma source employing nonlinear processes that occur in the plasma resonance region, in which the density of a nonuniform plasma is close to the critical density of an unmagnetized plasma, $n_{ec} = \frac{m(\omega_0^2 + \nu_{\text{eff}}^2)}{4\pi e^2}$ [1], where ω_0 is the microwave circular frequency and ν_{eff} is the effective electron–neutral collision frequency.

In a narrow region around the resonance surface, the microwave energy can be efficiently absorbed and converted into the kinetic energy of plasma electrons. The generation of accelerated electrons in plasma under the action of an intense electromagnetic field is a fundamental phenomenon, which has been thoroughly investigated both experimentally and theoretically (see, e.g., [2–4]). It should be noted that most of the studies on this subject were concerned with an inhomogeneous plasma in a highly rarified gas, in which the generation of fast electrons in the resonance layer and their escape into the surrounding medium can be analyzed without allowance for the interaction between electrons and gas molecules (atoms).

In the present work, we attempted to create conditions under which the energy of the electrons accelerated in the plasma resonance region was primarily spent on gas ionization, thereby leading to the formation of a plasma halo around this region.

In gas-discharge applications concerned with the plasma resonance phenomenon, the main variable parameter is the gas pressure, which should be low enough for the resonance not to be suppressed but, at the same time, should be high enough for ionization processes in the gas surrounding the resonance region to come into play.

In our experiments, the resonant mechanism for plasma production was studied using a coaxial microwave plasmatron similar to the Duo-Plasmaline system designed and investigated in [5]. A version of this system with one microwave source and a specially designed section for the output of microwaves from a coaxial waveguide was constructed and investigated at the Prokhorov Institute of General Physics of the Russian Academy of Sciences (see [6, 7]). The gas-discharge sources described in [5–7] can operate over a wide range of working gas pressures and are capable of producing cylindrical plasma layers with a plasma density higher than the critical value.

It is worth noting that the resonance phenomenon has long been utilized in devices based on the electron cyclotron resonance (ECR) in a magnetized plasma, at which the microwave circular frequency coincides with the electron cyclotron frequency, $\omega_c = \omega_0$ (see, e.g., [8, 9]). ECR discharges, however, have limited applications because the need to apply strong magnetic fields to the discharge region substantially complicates the plasmatron design and raises its cost.

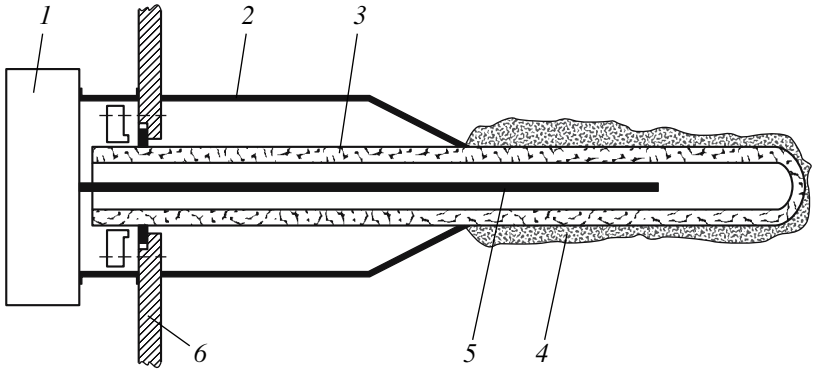

Fig. 1. Schematic of the coaxial microwave plasmatron: (*1*) magnetron, (*2*) outer electrode, (*3*) quartz tube, (*4*) plasma, (*5*) inner rod electrode, and (*6*) reactor chamber wall.

2. DESIGN OF A COAXIAL MICROWAVE PLASMA SOURCE AND SCHEME OF THE EXPERIMENT

A schematic of the coaxial microwave plasma source designed at the Institute of General Physics is shown in Fig. 1. Microwave radiation from magnetron *1* is fed to a coaxial waveguide consisting of outer cylindrical electrode *2* and inner rod electrode *5*. The inner electrode is inserted into quartz tube *3*, which is welded on the side of vacuum chamber *6*. The outer electrode is shorter than the inner electrode, which reaches the end of the quartz tube. The end of the outer electrode has the shape of a truncated cone, and its sharp edge is tightly adjacent to the surface of the quartz tube. The quartz tube extends out of the truncated outer electrode over a length of $L_{qt} \approx 10$–15 cm. The tube diameter is $\Theta_{qt} \approx 1.2$–1.5 cm. The diameter of the outer electrode of the coaxial waveguide (upstream of the conical transition to the quartz tube) is $\Theta_{ee} \approx 2.0$–2.5 cm.

After the magnetron is switched on, gas-discharge plasma *4* is produced near the surface of the gas-filled quartz tube around the extending part of the rod electrode.

Figure 2 shows a typical photograph of the operating coaxial microwave plasma source.

As a microwave source, we used a commercial magnetron commonly employed in domestic microwave ovens. The microwave wavelength was $\lambda_f \cong 12.5$ cm, and the mean microwave power was $\bar{P} \leq 1$ kW. The magnetron generated a train of microwave pulses with a duration of $\tau_f \cong 8$ ms, the time interval between pulses being $\Delta\tau \cong 12$ ms.

A schematic of the experimental setup used to study the plasma produced by the coaxial microwave source is shown in Fig. 3.

Plasmatron *1* (see Fig. 1) was introduced into cylindrical metal chamber *5* of diameter $\Theta_{ch} \cong 350$ mm. The chamber was pumped out to high vacuum and was filled with a working gas (argon) to a pressure of $0.02 \leq p \leq 5$ Torr. The chamber had two opposite quartz windows *8*, through which the diagnostic beam of a microwave interferometer operating at a wavelength of $\lambda_d \cong 8$ mm was input and output. Horn–lens antennas *2* and *3* were used to launch and receive the diagnostic beam. The interferometer measured the electron density in the plasma produced by the coaxial plasma source.

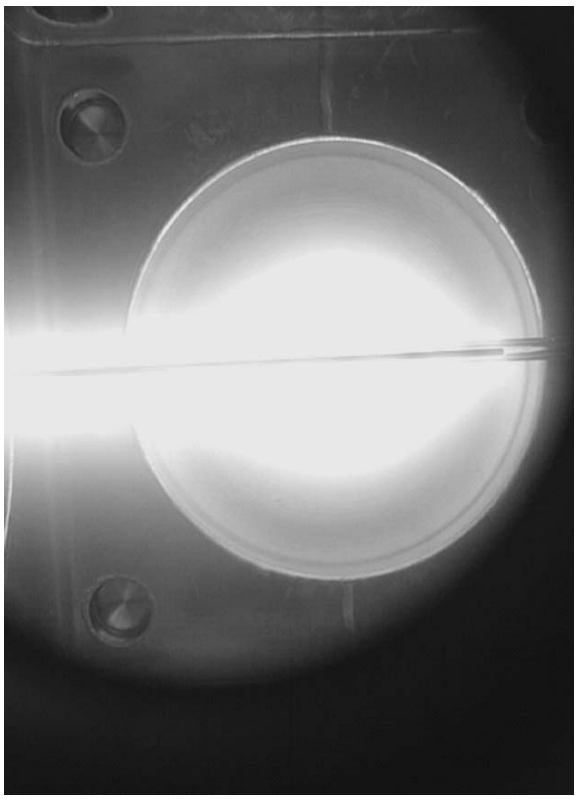

Fig. 2. Photograph of an operating coaxial microwave plasmatron.

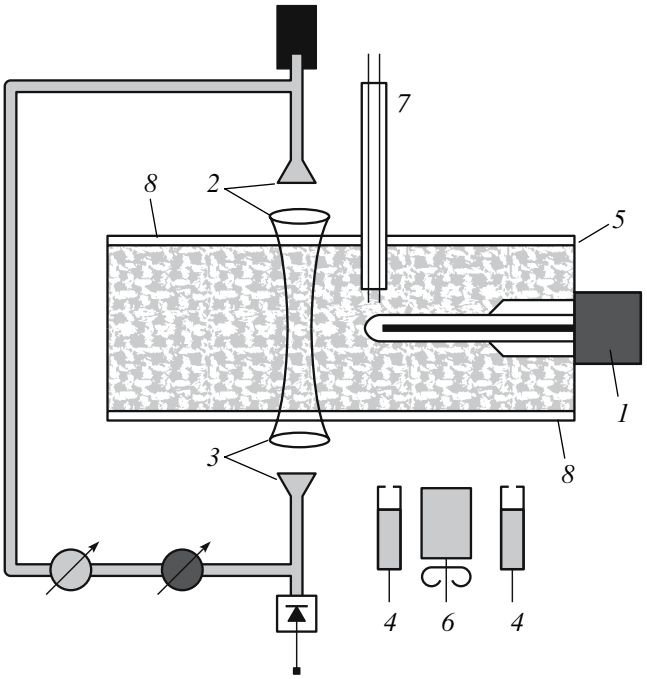

Fig. 3. Scheme of the experiment: (*1*) plasmatron, (*2*, *3*) horn–lens antenna of the microwave interferometer, (*4*) photomultiplier, (*5*) reactor vacuum chamber, (*6*) FER-7, (*7*) Langmuir probe, and (*8*) quartz windows.

The electron density was also measured by a double and a single Langmuir probe. The single probe was also used to measure the plasma potential.

The radial distribution of the plasma glow was measured by collimated photomultipliers *4*.

The dynamics of plasma propagation along the quartz tube during a microwave pulse was studied with the help of an FER-7 streak camera.

3. EXPERIMENTAL RESULTS

The plasma density in the chamber was measured using a diagnostic microwave beam by the scheme shown in Fig. 3. The working-gas (argon) pressure was varied in the range $0.02 \le p \le 1.0$ Torr. Under our experimental conditions ($\frac{\nu_{\text{eff}}}{\omega_d} \ll 1$ and $\frac{\bar{n}_e}{n_{ec}^d} \ll 1$, where ν_{eff} is the effective electron–neutral collision frequency and $\bar{n}_e$ is the plasma electron density averaged over the path length of the diagnostic beam), the value of $\bar{n}_e$ was determined from the following expressions for the phase shift ϑ and attenuation of the passed diagnostic beam [10]:

$$\Delta\vartheta = \left(\frac{\bar{n}_e}{n_{ec}^d}\right)\left(\frac{L}{\lambda_d}\right)\pi, \qquad (1)$$

$$\ln\left[\frac{I(0)}{I(L)}\right] = 2\pi\left(\frac{\bar{n}_e}{n_{ec}^d}\right)\left(\frac{L}{\lambda_d}\right)\left(\frac{\nu_{\text{eff}}}{\omega_d}\right). \qquad (2)$$

Here, L is the path length of the diagnostic microwave beam in the plasma; ω_d and λ_d are the circular frequency and wavelength of the diagnostic beam; $I(0)$ and $I(L)$ are the intensities of the diagnostic radiation at the input to and output from the plasma, respectively; and $n_{ec}^d = \frac{m_e(\omega_d^2 + \nu_{\text{eff}}^2)}{4\pi e^2}$ is the critical electron density for the diagnostic radiation.

Figure 4 shows typical signals from the phase detector of the microwave interferometer and from the photomultiplier recording plasma radiation.

The results of measurements of the density $\bar{n}_e$ are presented in Fig. 5. The diagnostic beam was displaced by 2 cm from the end of the quartz tube of the microwave plasma source.

In measurements performed with the single and double probes, the plasma density was calculated by the formula

$$n_e \cong \frac{4I_i}{eV_iS_p}, \qquad (3)$$

where I_i is the probe ion saturation current, S_p is the probe surface area, and $V_i \cong \sqrt{\frac{3kT_e}{2M_i}}$.

Figure 6 shows the dependence $n_e(p)$ measured by the probes at a distance of $r \cong 6.0$ cm from the axis. The radial density profile $n_e(r)$ measured by the probes at a pressure of $p = 0.1$ Torr is presented in Fig. 7. The measurements performed with the single probe at $p = 0.1$ Torr show that, 1–2 ms after the beginning of the microwave pulse, the electron temperature reaches 10–12 eV.

When considering the validity of probe measurements in these experiments, it should be remembered that, according to the results presented in [5] and obtained in our study, the microwave intensity decreases rapidly with distance away from the plasmatron axis. However, the most convincing argument in favor of the validity of probes measurements is that the electron density measure by the probes agrees well with that measured by microwave interferometry.

It can be seen from photographs that the microwave discharge is attached to the quartz tube and extends over the entire open surface of the tube, from the truncated outer electrode up to the tube end (more precisely, up to the end of the inner electrode of the coaxial waveguide). The transverse size of the plasma layer decreases with increasing working-gas pressure.

The thickness of the plasma layer can be inferred from measurements performed with collimated photomultipliers displaced in the direction orthogonal to the

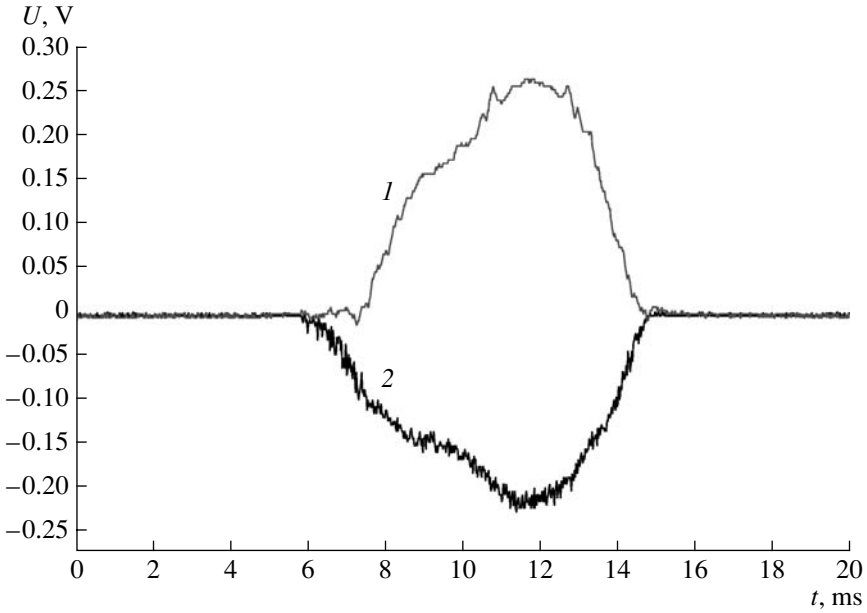

Fig. 4. Typical signals from the (*1*) microwave interferometer and (*2*) photomultiplier.

source axis at different distances from the end of the outer electrode. A typical distribution of the plasma glow intensity measured with a photomultiplier at p = 0.1 Torr is presented in Fig. 8.

Figure 9 presents plasma images obtained with the help of the FER-7 streak camera. The slit of the streak camera was oriented along the plasmatron axis and extended over the entire open area of the quartz tube, from the end of the truncated outer electrode up to the end of the inner electrode. The time and the z coordinate are plotted on the abscissa and ordinate, respectively. The time and spatial scales are indicated in the figure.

Figures 10 and 11 show the waveforms of the discharge glow intensity (lower curve) and the floating potential of the single probe (upper curve) at p = 0.1 and 1.0 Torr, respectively.

Figures 12 and 13 show the radial distributions of the floating potential of the single probe at different instants. The discharge was excited in argon at a pressure of 0.1 (Fig. 12) and 1.0 Torr (Fig. 13). Since the actual plasma potential φ_p exceeds the floating potential ($\varphi_p > \varphi_f$), it can be inferred from Figs. 12 and 13 that $\varphi_p \geq 75$ V for $p = 0.1$ Torr and $\varphi_p \geq 15$ V for $p = 1.0$ Torr. The dependence $\varphi_f(p)$ is presented in Fig. 6.

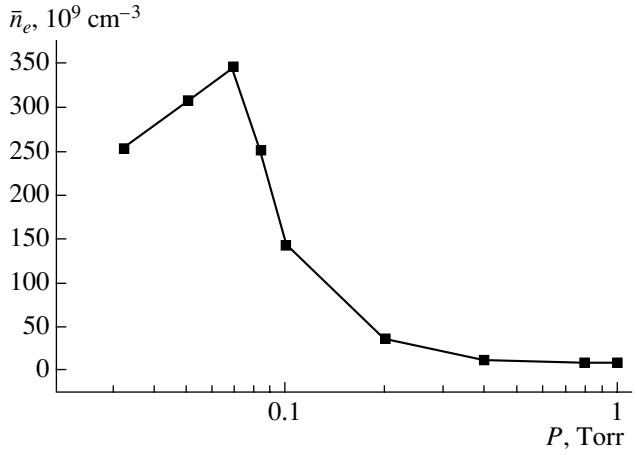

Fig. 5. Electron density averaged over the path length of the diagnostic beam as a function of the argon pressure ($\Delta z \cong$ 2 cm).

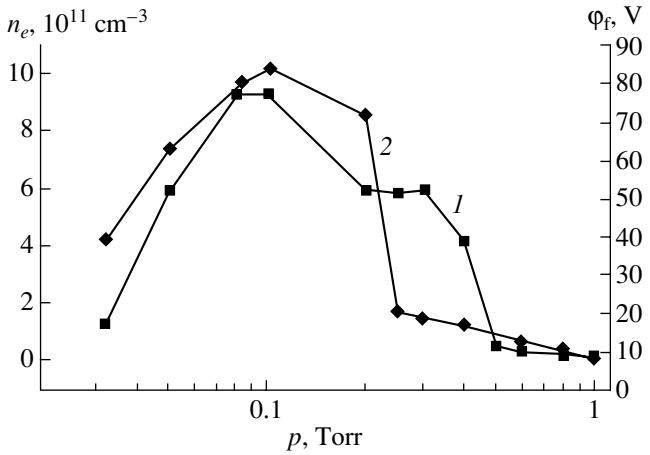

Fig. 6. (*1*) Electron density measured by the Langmuir probe and (*2*) floating potential of the probe as functions of the argon pressure in the chamber.

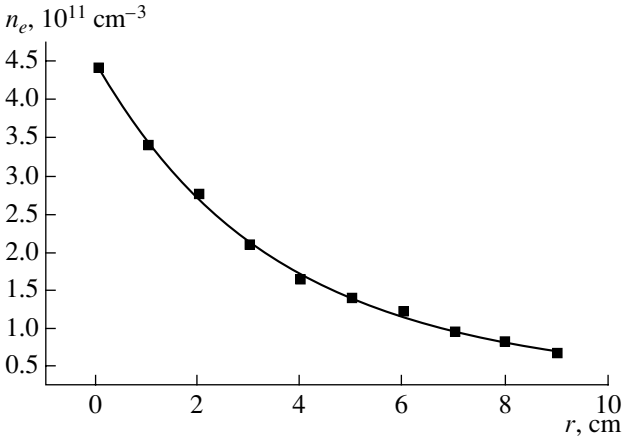

Fig. 7. Radial profile of the electron density for p = 0.05 Torr and $\Delta z \cong 0.3$ cm. The experimental points are fitted by the dependence $n_e/10^{11} = 0.35 + 4.06\exp(-r/3.68)$ (solid line).

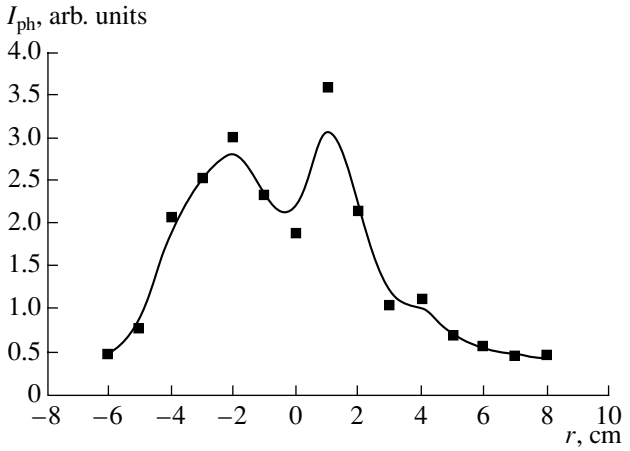

Fig. 8. Radial profile of the radiation intensity from a microwave discharge excited in argon at a pressure of $p = 0.1$ Torr ($t = 5$ ms). The coordinate $r = 0$ corresponds to the axis of the coaxial plasmatron.

4. DISCUSSION OF THE EXPERIMENTAL RESULTS

The results of our experiments indicate that, at relatively low argon pressures, the plasma parameters in the microwave gas-discharge source under study are governed by the nonlinear processes occurring in the plasma resonance region. This is confirmed, in particular, by the very large values of the electron density, temperature, and plasma potential that cannot be explained by the conventional models of a microwave discharge (see, e.g., [11, 12]): $n_e \geq 3 \times 10^{11}$ cm$^{-3} \gg n_{ec} \approx 6.4 \times 10^{10}$ cm^{-3}, $T_e \geq 10$–12 eV, and $\varphi_p \geq 70$ V.

To explain such high values of the plasma parameters, it is necessary to assume that, immediately near the plasmatron, there is a resonance layer in which the microwave energy is efficiently converted into the electron energy.

The conditions under which an electromagnetic wave can interact nonlinearly with an inhomogeneous plasma are schematically illustrated in Fig. 14. The electromagnetic wave is efficiently absorbed and the plasma electrons are accelerated within a narrow plasma layer adjacent to the resonance surface, at which the electron density is equal to the critical density. The theory attributes the generation of fast electrons with energies far exceeding the thermal energy (such a generation was observed experimentally, e.g., in [13–15]) to the considerable enhancement of the electric field in the plasma resonance region in an inhomogeneous plasma. The electrons interacting with such a localized microwave field can acquire energy via collisions [16], due to the Cherenkov resonance acceleration [17], or as a result of wavebreaking of nonlinear plasma oscillations in a strong pump field [18, 19]. If the ion density profile is nearly linear, the electrons in the plasma resonance region are primarily accelerated toward the lower plasma density.

A necessary condition for the strongly nonlinear interaction of an electromagnetic wave with an overcritical inhomogeneous plasma is the presence of the electric field component parallel to the plasma density gradient.

The main parameters characterizing the plasma resonance region can be estimated using the existing theory of the plasma resonance (see, e.g., [4, 20]).

Thus, the width of the resonance region is determined by the formula

$$\Delta R_{\text{res}} \approx R_p S, \tag{4}$$

the amplitude of the enhanced electric field in this region is

$$\tilde{E}_{\text{res}} \approx \frac{\tilde{E}_{0r}}{S}, \tag{5}$$

and the characteristic energy of fast electrons generated in the resonance region in the collisionless regime can be estimated as

$$\varepsilon_{eh} \sim eE_{0r}R_p. \tag{6}$$

In Eqs. (4) and (5), the parameter S is equal to the maximum of the three dimensionless quantities,

$$S = \max\left\{\left(\frac{\nu_{\text{eff}}}{\omega_0}\right); \left(\frac{r_{De}}{R_p}\right)^{2/3}; \left(\frac{r_{\text{osc}}}{R_p}\right)^{1/2}\right\}, \tag{7}$$

where R_p is the characteristic scale length of the plasma inhomogeneity, λ is the microwave wavelength, r_{De} is the Debye radius, r_{osc} is the amplitude of electron oscillations in the plasma resonance, and $\tilde{E}_{0r}$ is the amplitude of the radial component of the vacuum electric field of the electromagnetic pump wave.

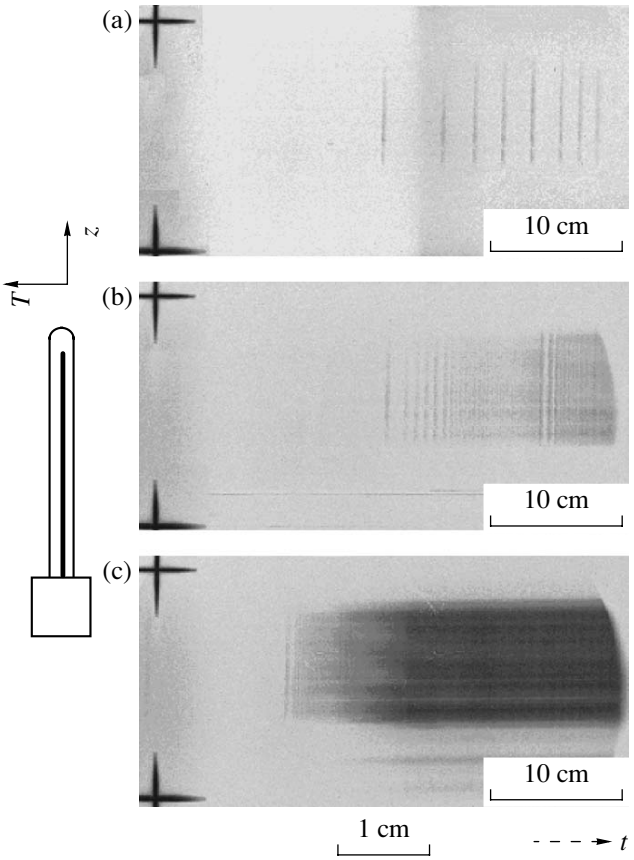

Fig. 9. Streak images obtained with the help of the FER-7 streak camera. The entrance slit is oriented along the z axis. A microwave discharge was excited in argon at a pressure of p = 1.0 Torr. The time scale is (a) 75, (b) 250, and (c) 750 μs/cm.

Turning to the experimental results described in this paper, we note that almost all of the necessary conditions for the plasma resonance are satisfied at pressures $p \ll 1$ Torr. The electron density near the plasmatron well exceeds the critical density and, at a certain distance r_c, from the source takes the value n_{ec}. If the electron density reaches its maximum value at a certain distance from the surface of the quartz tube, then the radial profile of the density n_e may have two points at which $n_e = n_{ec}$, one lying on the plasmatron side and the other lying on the chamber-wall side. This means that there may be a resonance region (or two such regions) within which the density gradient is directed radially, i.e., is orthogonal to the plasmatron axis. The electric field of the electromagnetic wave emitted from the plasmatron also possesses the radial component $\tilde{E}_{0r}$. This is confirmed, in particular, by the numerical simulations performed using the KARAT code [21]. Figures 15 and 16 show a typical calculated distribution of the electric field of the electromagnetic wave emitted from the plasmatron in the prebreakdown phase (the vacuum field in the absence of a plasma). Figures 17 and 18 show the distribution of the electric field calculated under the assumption that, near the surface of the quartz tube, there is a plasma layer with the critical density at $r \cong$ 1.0 cm.

It should be noted that the presence of a substantial radial component of the electric field $\tilde{E}_{0r}$ near the dielectric tube in the plasmatron under study (as well as in the Duo-Plasmaline system [5]) is related to the specific design of the microwave energy output from the coaxial waveguide. Conventional configurations in which the plasma is produced inside a dielectric tube

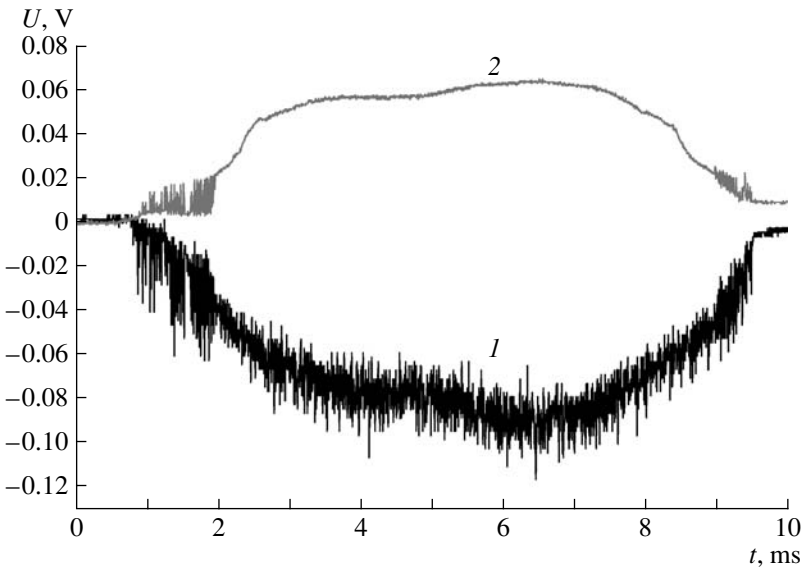

Fig. 10. Waveforms of the (*1*) plasma radiation intensity and (*2*) floating potential of the Langmuir probe. A microwave discharge was excited in argon at a pressure of p = 0.1 Torr. The floating potential was recorded using a 1 : 1000 voltage divider.

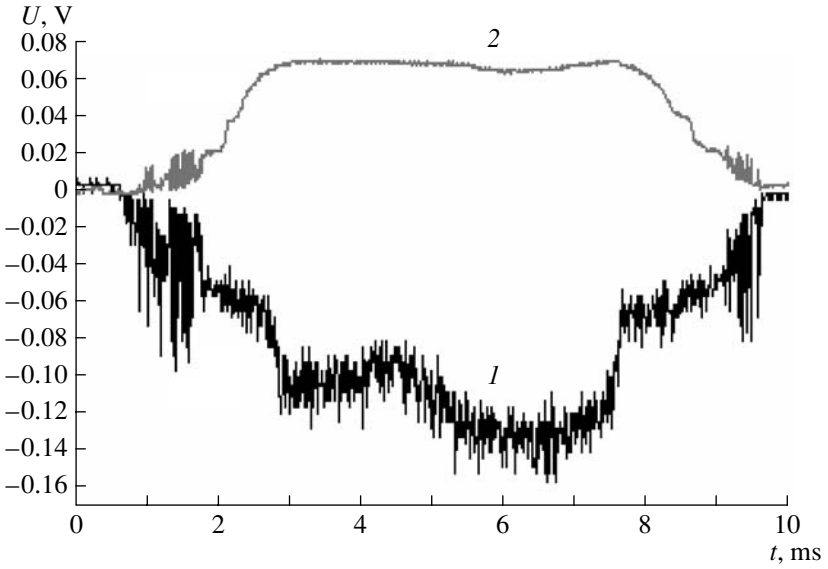

Fig. 11 The same as in Fig. 10, but at a pressure of $p = 1.0$ Torr.

(the so-called configurations with an "internal surface wave" [5]) fail to produce a substantial component $\tilde{E}_{0r}$ and, therefore, do not satisfy the conditions necessary for electron acceleration (heating) in the plasma resonance region.

An electromagnetic wave propagating in the radial direction down the plasma density gradient penetrates into a plasma to a depth on the order of

$$\delta \approx \frac{c}{\omega_p}, \tag{8}$$

which under our experimental conditions amounts to a few centimeters and is comparable with the characteristic radial size of the plasma layer. This means that the nonlinear interaction of the electromagnetic wave with the plasma can occur on both the inner and outer slops of the electron density profile.

Our experiments were performed at argon pressures satisfying the inequality $\nu_{\text{eff}} < \omega_0$, which is a necessary condition for the occurrence of resonance processes. (Using the approximate relationship for argon [11], $\nu_{\text{eff}} \cong 7 \times 10^9 p$, where p is in Torr, we find that strong resonance effects can occur at pressures $p \ll 2$ Torr.)

Under our experimental conditions, the parameter S, characterizing the intensity of nonlinear processes in the resonance region, is equal to the ratio $\frac{\nu_{\text{eff}}}{\omega_0}$ and, at $p = 0.1$ Torr, amounts to $S \approx 5 \times 10^{-2}$.

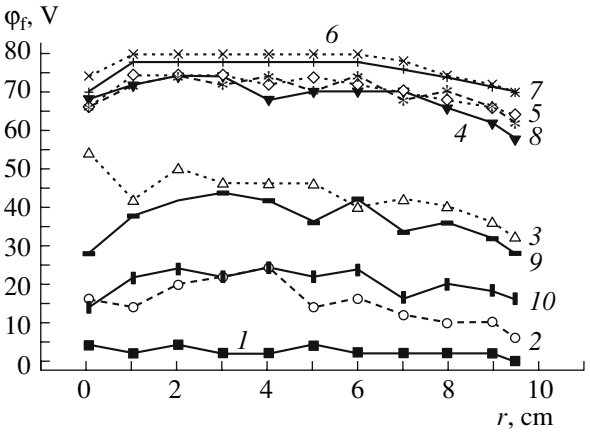

Fig. 12. Radial profile of the floating potential of the Langmuir probe at successive instants: (*1*) 1, (*2*) 2, (*3*) 3, (*4*) 4, (*5*) 5, (*6*) 6, (*7*) 7, (*8*) 8, (*9*) 9, and (*10*) 10 ms. A microwave discharge was excited in argon at a pressure of $p = 0.1$ Torr.

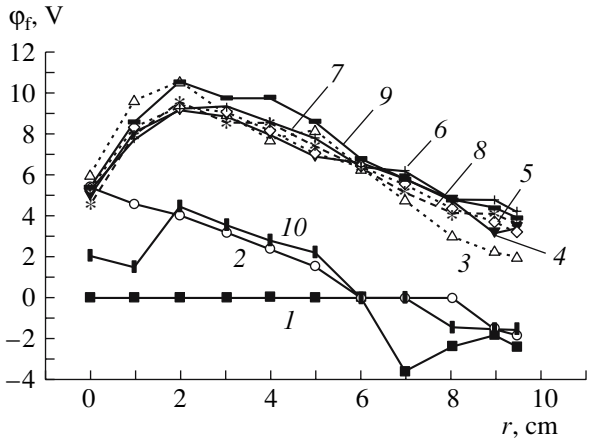

Fig. 13. The same as in Fig. 12, but at a pressure of $p = 1.0$ Torr.

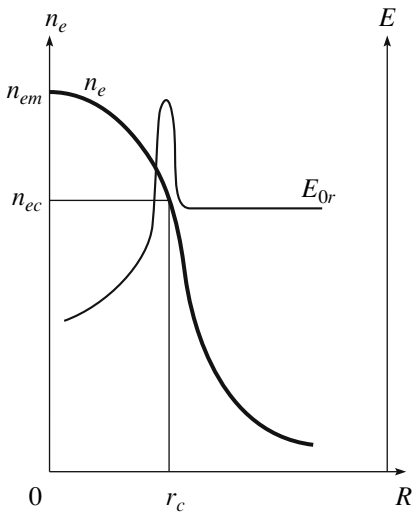

Fig. 14. Schematic representation of the plasma resonance in an inhomogeneous plasma.

In our experiments, we have $R_p \cong (1–2)$ cm; therefore, the width of the discharge region (see Eq. (4)) is equal to $\Delta R_{\text{res}} \approx (0.05–0.1)$ cm.

According to Fig. 16, the radial component of the vacuum microwave electric field at $z = 5$ cm does not exceed $\tilde{E}_{0r} \approx 100$ V/cm. It then follows from Eq. (5) that the enhanced electric field in the resonance region is $\tilde{E}_{\text{res}} \approx 2 \times 10^3$ V/cm.

From Eq. (6), we find that the energy of fast electrons generated in the resonance region is $\varepsilon_{eh} \approx 80$ eV.

At p =1.0 Torr and $z = 5$ cm, we have $S \approx 0.5$. This means that $\Delta R_{\text{res}} \approx 1$ cm and $\tilde{E}_{\text{res}} \approx 200$ V/cm. The electron mean free path at this pressure is $l_e \approx \dfrac{1}{n_m \sigma} \approx 3 \times 10^{-2}$ cm (where σ is the cross section for elastic electron scattering), which is much smaller than the width of the resonance region, and the enhanced field $\tilde{E}_{\text{res}}$ differs only slightly from the vacuum field. Under these conditions, the average energy (or temperature) acquired by the electrons in the resonance region can be estimated using conventional models [11, 12] by the formula

$$T_{e\,\text{res}} \approx \frac{\tilde{E}_{\text{res}}^2 e^2}{3 m_e \eta_e (\omega_0^2 + \nu_{\text{eff}}^2)}, \tag{9}$$

where η_e is the energy fraction lost by an electron in a collision event with a neutral particle. For the reduced electric field $\dfrac{\tilde{E}_{\text{res}}}{n_m}$ typical of our experiments, we have $\eta_e \approx 0.1–1$ [11, 12]. Using these values of η_e, we find that the average energy acquired by the electrons in the resonance region is on the order of $T_{er} \approx 0.1–1$ eV, which is much smaller than the energy of electrons accelerated in the resonance region at low argon pressures ($\varepsilon_{eh} \approx 80$ eV for $p = 0.1$ Torr).

The fast electrons that are generated in the resonance region and then are accelerated down the plasma density gradient can lose their energy in collisions with neutral particles, thereby ionizing the gas in the cham-

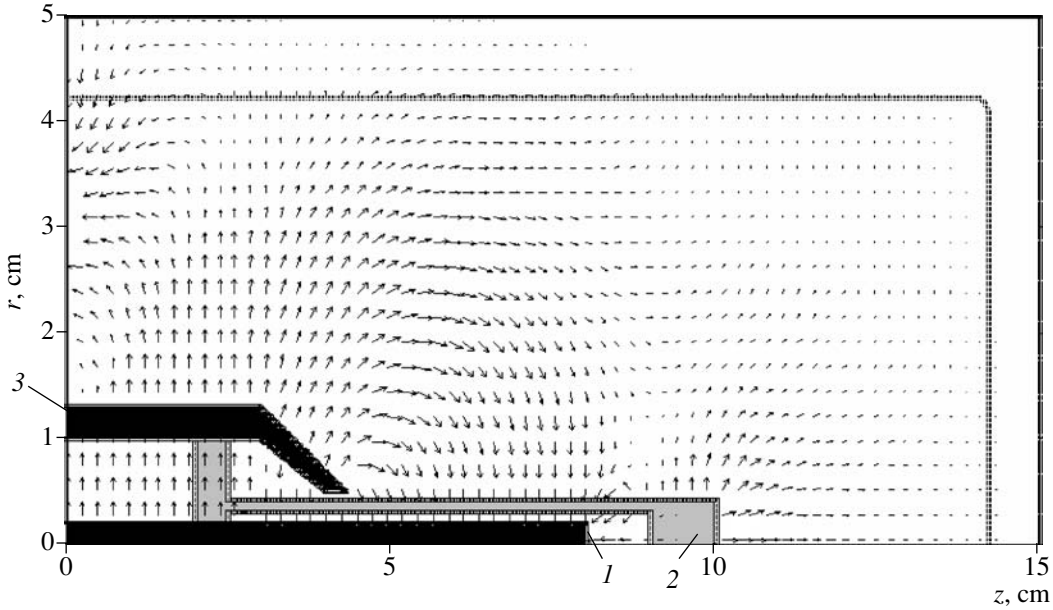

Fig. 15. Calculated spatial distribution of the microwave electric field in a coaxial plasmatron in the prebreakdown stage: (*1*) central electrode of the coaxial waveguide, (*2*) dielectric tube, and (*3*) outer electrode of the coaxial waveguide.

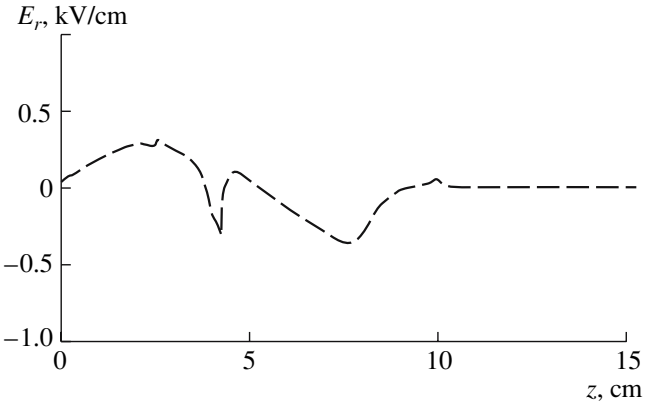

Fig. 16. Calculated longitudinal distribution of the radial component of the microwave electric field at the outlet from a coaxial plasmatron ($r = 0.5$ cm).

ber volume. The characteristic mean free path of fast electrons ($\varepsilon_{eh} \cong 80$ eV) with respect to ionizing collisions at an argon pressure of $p \cong 0.1$ Torr is

$$l_i \approx \frac{1}{n_m \sigma_i} \approx 1 \text{ cm} \ll R_c, \qquad (10)$$

where σ_i is the ionization cross section (which, for $\varepsilon_{eh} \approx 80$ eV, is on the order of $\sigma_i \approx 3.5 \times 10^{16}$ cm^{-2} [11]) and R_c is the chamber radius.

The volume ionization can also be produced by the UV radiation generated on the quartz tube surface bombarded by the electrons reflected from the potential barrier formed by the quasistatic charge-separation field in the plasma. In this case, step photoexcitation can substantially contribute to photoionization [22].

Thus, in our experiments, a situation can occur in which electrons are accelerated in the collisionless regime to energies on the order of 100 eV within a narrow resonance region and then efficiently expend this energy on gas ionization in the chamber volume outside the resonance region.

The concept involving the processes occurring in the plasma resonance region agrees with many of our experimental results. First of all, this is an increase in the electron density and plasma potential with decreasing gas pressure. It follows from the above analysis that such an increase can be caused by a decrease in the ratio $\frac{\nu_{\text{eff}}}{\omega_0}$ and, hence, by an increase in the electric field and, accordingly, in the energy acquired by the electrons in the resonance region. It was found experimentally (see, e.g., [2, 13]) that the energy distribution function (EDF) of the electrons that have passed through the resonance region contains a group (or groups) of high-energy electrons (beams) whose energy is determined by expression (6). In addition, the EDF is characterized by the high temperature of the bulk electrons. (The high temperature is a result of the high effective collision frequency, which is caused by the onset of plasma instabilities in the resonance region and is substantially higher than the frequencies of electron–neutral and electron–ion collisions.)

Depending on which component makes the main contribution to the electron flux toward the chamber wall, the plasma potential can be determined by either the temperature of the Maxwellian part of the electron energy distribution [11],

$$\varphi_p \approx \frac{kT_{e\,\text{res}}}{e} \ln \sqrt{\frac{M_i}{m_e}}, \qquad (1)$$

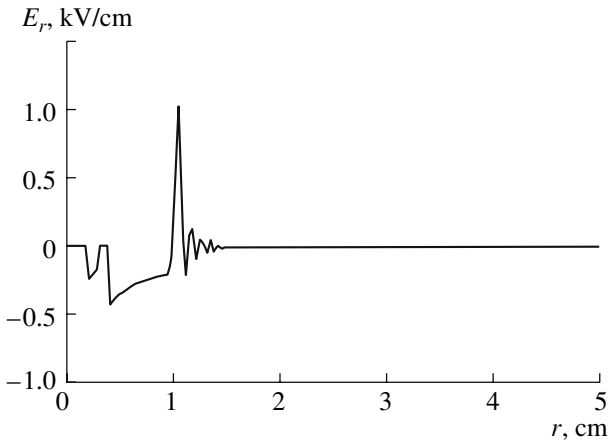

Fig. 17. Calculated distribution of the radial component of the microwave electric field at the outlet from a coaxial plasmatron in the presence of a plasma layer near the surface of the quartz tube ($z = 5.0$ cm).

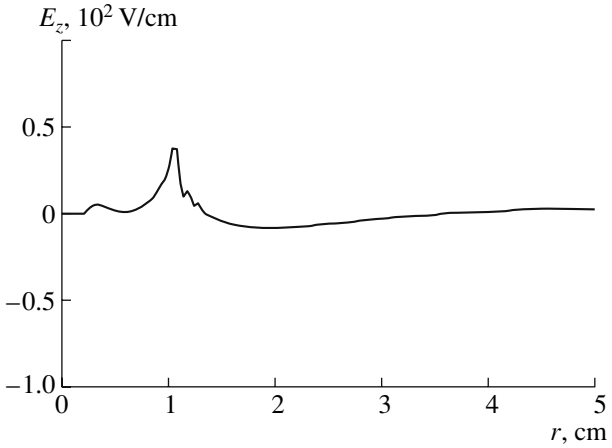

Fig. 18. Calculated distribution of the axial component of the microwave electric field at the outlet from a coaxial plasmatron in the presence of a plasma layer near the surface of the quartz tube ($z = 5.0$ cm).

regime to energies on the order of 100 eV within a narrow resonance region and then efficiently expend this energy on gas ionization in the chamber volume outside the resonance region.

The concept involving the processes occurring in the plasma resonance region agrees with many of our experimental results. First of all, this is an increase in the electron density and plasma potential with decreasing gas pressure. It follows from the above analysis that such an increase can be caused by a decrease in the ratio $\frac{\nu_{\text{eff}}}{\omega_0}$ and, hence, by an increase in the electric field and, accordingly, in the energy acquired by the electrons in the resonance region. It was found experimentally (see, e.g., [2, 13]) that the energy distribution function (EDF) of the electrons that have passed through the resonance region contains a group (or groups) of high-energy electrons (beams) whose energy is determined by expression (6). In addition, the EDF is characterized by the high temperature of the bulk electrons. (The high temperature is a result of the high effective collision frequency, which is caused by the onset of plasma instabilities in the resonance region and is substantially higher than the frequencies of electron–neutral and electron–ion collisions.)

Depending on which component makes the main contribution to the electron flux toward the chamber wall, the plasma potential can be determined by either the temperature of the Maxwellian part of the electron energy distribution [11],

$$\varphi_p \approx \frac{kT_{e\,\text{res}}}{e} \ln \sqrt{\frac{M_i}{m_e}}, \tag{11}$$

or the energy of the fast electron beam

$$\varphi_p \approx \frac{\varepsilon_{eh}}{e}. \tag{12}$$

The measured electron temperature and the calculated (from expressions (6) and (9)) values of ε_{eh} and $T_{e\,\text{res}}$ are consistent with both the value of the plasma potential measured by probes and its dependence on the working-gas pressure. At relatively low pressures (when the resonant phenomena are most pronounced), the collision frequency ν_{eff} entering into expression (9) is the frequency of electron scattering by Langmuir plasma waves. According to [23], this frequency can be very high: $\nu_{ei}, \omega_{pi} \ll \nu_{\text{eff}} \leq \omega_{pe}$, where ν_{ei} is the electron–ion collision frequency, ω_{pi} is the plasma ion frequency, and ω_{pe} is the plasma electron frequency.

Our concept is also consistent with the observed time evolution of the electron density n_e and the probe floating potential φ_f (see Figs. 4, 10, and 11). The time evolution of n_e and φ_f is characterized by the time delay $\Delta t \cong$ (1–2) ms between the beginning of the microwave pulse (which approximately coincides with the appearance of the plasma glow detected by the photomultiplier) and the rapid growth of the plasma density and the plasma potential. Probe measurements show that the growth of the electron temperature is delayed by nearly the same time interval. An analysis of the photomultiplier signals and streak images of the discharge indicates that the plasma layer forms around the entire open surface of the quartz tube over a time shorter than the time by which the growth of n_e, T_e, and φ_p is delayed. The observed time delay may be interpreted as the time it takes for the electron density in the formed plasma layer to increase above the critical value, after which a resonance region (or regions) with an enhanced electric field appears in the plasma.

From Fig. 6, which presents the results of probe measurements of the electron density and plasma potential, it follows that the nonlinear interaction of the microwave field with the plasma in the resonance region manifests itself at argon pressures from $p \cong 0.5$ Torr to $p \cong 0.03$ Torr. It should be noted, however, that not all of the experimental results obtained in the present work can be explained by the theory of the plasma resonance (see, e.g., [3, 4]). To develop an adequate physical model of a microwave plasmatron, it is necessary to take into account the specific features of the plasma source under study, first of all, the specific character of the initiation and formation of the primary plasma layer. Thus, a decrease in n_e and φ_f at pressures below $p < 0.1$ Torr may be attributed to the worse conditions for gas breakdown on the left branch of the breakdown curve (an analogue of the Paschen curve). It should be noted that, when operating with this type of coaxial plasmatron, the plasma is generated only at pressures $p \geq 0.02$ Torr.

The problem of the initiation and formation of a primary plasma layer near the quartz tube is of particular interest and calls for special investigations. In reconstructing a physical picture describing the initiation processes, we should take into account the specific character of the initial phase of the discharge, which manifests itself in streak images (see Fig. 9) as a sequence of plasma bursts generated at a rate of $f \geq 20$ kHz. Such a bursty character of plasma generation in the early stage of the discharge may be attributed to the specific features of magnetron operation (see [24]). The matter is that, in the initial stage of its operation, the magnetron first produces a sequence of short ($\tau \leq 100$ ns) high-power ($f \geq 20$ kHz) pulses with a repetition rate of $P \geq 20$ kW and, after a certain time period, reaches its standard operating regime with a pulse duration of $\tau \cong 8$ ms and repetition rate of $f \cong 50$ Hz.

When considering the nonlinear interaction of microwave radiation with the gas-discharge plasma produced by this radiation, it is necessary to take into account the results of [25, 26], where the possible role of the plasma resonance in the formation of a gas discharge was pointed out. Unfortunately, the transformation of the microwave energy into the energy of plasma electrons and the role of the accelerated electrons in the

ionization processes outside the overcritical plasma layer remained beyond the scope of these very interesting works.

5. CONCLUSIONS

The results of our experiments indicate that we have managed to create conditions under which the parameters of the plasma produced in the reactor chamber of a microwave plasmatron are governed by the nonlinear processes occurring in the plasma resonance region. That the nonlinear interaction of an electromagnetic wave with the inhomogeneous plasma created by this wave is efficient is evidenced by the high electron density n_e and high plasma potential φ_p achieved in the plasmatron at working gas (argon) pressures of $0.03 \le p \le 0.5$ Torr. In most of this pressure range, the plasma density at a distance of a few centimeters from the plasmatron is substantially (by a factor of 3–5) higher than the critical density for the microwaves exciting the discharge. The electron temperature in this case reaches $T_e \cong 10$–12 eV.

Fast electrons and UV radiation generated in the resonance region can serve as ionization sources in the plasmatron chamber.

The resonance microwave plasma source described in this paper can be used in various applications, in particular, in plasma chemistry (e.g., for dry etching of large semiconductor plates), in developing gas-discharge sources of visible light and UV radiation, etc.

ACKNOWLEDGMENTS

We thank G.M. Batanov and V.P. Silakov for very helpful discussions. This work was supported by the Samsung Electronics Co., LTD; the Netherlands Organization for Scientific Research (project NWO 047.016.019); and the RF Presidential Program for Support of Leading Scientific Schools (project no. NSh-5382.2006.2).

REFERENCES

1. V. L. Ginzburg, *The Propagation of Electromagnetic Waves in Plasmas* (Nauka, Moscow, 1967; Pergamon, Oxford, 1970).
2. *Plasma Physics and Plasma Electronics*, Ed. by L. M. Kovrizhnykh (Nauka, Moscow, 1985; Nova Science, Commack, NY, 1989).
3. *Dissipation of Electromagnetic Waves in Plasma* (Nauka, Moscow, 1977), Trudy FIAN **92** (1977).
4. *Generation of Nonlinear Waves and Quasi-Steady Currents in Plasma* (Nauka, Moscow, 1988), Trudy IOFAN **16** (1988).
5. E. Rauchle, J. Phys. France **8** (7), 99 (1998).
6. S. I. Gritsinin, I. A. Kossyi, N. I. Malykh, et al., Preprint No. 1 (Prokhorov Institute of General Physics, Moscow, 1999).
7. S. I. Gritsinin, I. A. Kossyi, N. I. Malykh, et al., in *Proceedings of the 14th International Symposium on Plasma Chemistry, Prague, 1999*, Ed. by M. Hrabovsky, M. Konrad, and V. Kopecky, Vol. 2, p. 675.
8. R. Geller, *Electron Cyclotron Resonance Ion Sources and ECR Plasmas* (IOP, Bristol, 1996).
9. R. Geller, Rev. Sci. Instrum. **69**, 1302 (1998).
10. V. E. Golant, *Microwave Methods in Plasma Studies* (Nauka, Moscow, 1968) [in Russian].
11. Yu. P. Raizer, *Gas Discharge Physics* (Nauka, Moscow, 1987; Springer-Verlag, Berlin, 1991).
12. A. D. MacDonald, *Microwave Breakdown in Gases* (Wiley, New York, 1966).
13. G. M. Batanov, N. K. Berezhetskaya, A. A. Dorofeyuk, et al., Fiz. Plazmy **9**, 604 (1983) [Sov. J. Plasma Phys. **9**, 352 (1983)].
14. P. De Neef, Phys. Rev. Lett. **39**, 997 (1977).
15. G. M. Batanov, V. A. Ivanov, and I. A. Kossyi, Fiz. Plazmy **12**, 552 (1986) [Sov. J. Plasma Phys. **12**, 317 (1986)].
16. S. V. Bulanov and L. M. Kovrizhnykh, Fiz. Plazmy **1**, 1016 (1975) [Sov. J. Plasma Phys. **1**, 555 (1975)].
17. L. M. Kovrizhnykh and A. S. Sakharov, Fiz. Plazmy **5**, 840 (1979) [Sov. J. Plasma Phys. **5**, 470 (1979)].
18. S. V. Bulanov, L. M. Kovrizhnykh, and A. S. Sakharov, Zh. Éksp. Teor. Fiz. **72**, 1809 (1977) [Sov. Phys. JETP **45**, 949 (1977)].
19. J. Albritton and P. Koch, Phys. Fluids **18**, 1136 (1975).
20. *Interaction of Strong Electromagnetic Waves with Collisionless Plasmas*, Ed. by A. G. Litvak (IPF AN SSSR, Gorki, 1980) [in Russian].
21. V. P. Tarakanov, *User's Manual for Code KARAT* (Berkley Research Associate, Springfield, 1992).
22. I. A. Kossyi and V. P. Silakov, Plasma Sources Sci. Technol. **14**, 594 (2005).
23. A. M. Anpilov, I. A. Kossyi, G. S. Luk'yanchikov, and P. O. Nikuradze, Zh. Tekh. Fiz. **55**, 2340 (1985) [Sov. Phys. Tech. Phys. **30**, 1390 (1985)].
24. S. I. Gritsinin, V. Yu. Knyazev, I. A. Kossyi, et al., Fiz. Plazmy **30**, 283 (2004) [Plasma Phys. Rep. **30**, 255 (2004)].
25. D. M. Karfidov, N. A. Lukina, and K. F. Sergeichev, in *Plasma Physics and Plasma Electronics*, Ed. by L. M. Kovrizhnykh (Nauka, Moscow, 1985; Nova Science, Commack, NY, 1989).
26. H. Sugai, I. Chanashev, and M. Nagatsu, Plasma Sources Sci. Technol. **7**, 192 (1988).

Translated by N.F. Larionova